BRUCE NGS: ASSESSMENT OF CALANDRIA TUBE INTEGRITY FOLLOWING A SUDDEN PRESSURE TUBE FAILURE.

P.S. Kundurpi, A.P. Muzumdar and F.B.P. Tran

Ontario Hydro, Toronto, Ontario.

Abstract

The issue of calandria tube integrity following a sudden rupture of the pressure tube in Bruce NGS is addressed in this paper. During this accident scenario, the CT is subjected to severe pressure and impact loading. The paper focuses on the transient stage in which the annulus pressure usually exceeds the header pressure due to a water-hammer type pressure transient. A detailed sensitivity study of the thermal-hydraulic response of the fuel channel and the gas annulus during the transient is presented. Based on this sensitivity study results, the margin to calandria tube failure is also evaluated.

INTRODUCTION

The main function of the calandria tube (CT) is to minimize the heat loss from the primary coolant, contained within the pressure tube (PT), to the cool moderator by providing an insulating annulus space. In Bruce NGS reactors, this provision is achieved by circulating dry CO_2 gas in the gas annulus system which also acts as a means of detecting any leaks in the pressure tubes. The calandria tubes are subjected to the internal pressure of the annulus gas and to the external pressure due to the moderator. They also take up a portion of the fuel channel weight.

Based on these functional and loading considerations the CTs are designed as ASME Class III pressure vessels. However, during accident scenarios involving PT rupture, the surrounding CT is subjected to severe pressure and impact loading depending on the nature of the PT failure. In the licensing analysis it is conservatively assumed that any pressure tube rupture also results in the rupture of the associated calandria tube. As the economic consequences of a PT rupture are much smaller if the CT survives, there is an incentive to evaluate the survivability of the CT in detail. Based on experimental observation, the previous investigations (Ref 1,2 and 3) have shown that the sequence of events following pressure tube failure can be delineated into three distinct stages ie., the initial transient annulus filling stage, the transient over-pressurisation stage and the final steady state pressurisation following bellows rupture.These investigations, which discussed the resulting interactions between the PT and the CT, have identified the annulus filling phase as very important for assessing CT response. Consequently this paper only considers the annulus filling stage in detail. The peak water-hammer pressures during the transients and the structural response of the CT to these transients is examined. Based on the results obtained, the paper presents the strength margins for survivability of CT in Bruce NGS A and B reactors due to a pressure tube failure.

THERMAL-HYDRAULIC RESPONSE

In this section, a sensitivity analysis of the thermal-hydraulic response of the fuel channel during the annulus fill-up stage is presented. In particular, attention is focused on the overpressure in the annulus caused by the surge of coolant following the pressure tube rupture. The magnitude of the pressure rise is essentially dependent upon the fluid discharge rate into the annulus which is determined by the header to header hydraulic resistance and upon the channel power. The pressure transients are evaluated assuming that the pressure boundary between the headers is rigid. In the present sensitivity study, the MINI-SOPHT computer code is used to evaluate the pressure transient using the rigid boundary assumption.

The main parameters considered in the sensitivity study are different break lengths, break locations (inlet end, outlet end, break over the entire length of the pressure tube), break discharge area, bearing clearances, channel power (inner and outer zone) and flow. Results obtained using MINI-SOPHT for a number of channels in Bruce A are reported. These results and the pressure pulse data are later used as input to assess calandria tube integrity.

Methodology and Assumption

The thermal-hydraulic behaviour of the channel/feeder system was simulated for a number of channels in the core. In particular four channels, two in the inner (high power) zone and two in the outer (low power) zone were selected for the analysis, i.e., Channel J09 and L10 in the high power region and K01 and A08 in the low power region. These channels were selected so as to combine the highest flow and the lowest power in each region resulting in the highest coolant subcooling.

The channel geometries are obtained from the NUCIRC code data files. The friction loss coefficient of various components in the MINI-SOPHT model are obtained by matching the pressure drop with that calculated using

NUCIRC at nominal conditions as well as other power levels. Table 1 shows the geometry data and nominal channel parameters (i.e., flow rate, power and inlet temperature) for the inner zone Channels J09 and for the outer zone Channels K01.

Figure 1 shows the schematic nodalization representing the header to header model to simulate the different pressure tube break scenarios. The pressure tube and the annulus are each represented by 13 nodes. Each pressure tube and annulus node are connected by two parallel break discharge valves to simulate the crack in the pressure tube. An outlet-end break, inlet-end break, full-length break or any length of break at any location can be simulated by opening the appropriate discharge valves. For all cases, the nominal break area is assumed to be 30 cm^2 per bundle length. Thus the total break area assumed for a full length break is 390 cm^2. The nominal break opening time of 10 ms is used in all the cases. The nominal bearing clearance is assumed to be 2.5 cm^2. The following additional general assumptions are used in the SOPHT simulations of the breaks:

(a) Two parallel break valves are used to connect the pressure tube node and the annulus node. One link is used to model the forward flow from the pressure tube to the annulus, and the other is used for the flow in the opposite direction.

(b) The break discharge flow from the pressure tube to the annulus and through the bearings are modelled using the Henry-Fauske orifice discharge model.

(c) The bellows are assumed to burst at 5 MPa and, hence, discharge through the bellows is activated when the pressure at the bellows node is approximately 5 MPa.

<u>Simulation Results</u>

With these main parameters and assumptions, a number of PT breaks have been simulated by MINI-SOPHT to study the effect of various parameters such as break length, channel power, etc. Table 2 shows the matrix of cases considered for the sensitivity analysis and the results of the sensitivity analysis. The following discussion of results highlights the effects of the major variables on the pressure transient in the gas annulus.

<u>Effect of Channel Power and Flow (Inner and Outer Zones)</u>

Figures 2 and 3 show the pressure transients in the annulus and the pressure tube for the inner zone Channel J09 and the outer zone Channel K01 at nominal channel conditions with a full-length break. For the high power Channel (J09), no water-hammer over pressurization is observed. For the low power Channel (K01) the maximum predicted pressure is 15 MPa and the duration of the pulse is approximately 55 ms. Similar results are predicted for Channels L10 and A08 in the high and low power regions respectively (cases 2 and 3 in Table 2). In general no water-hammer pressure transients are predicted in the high power channels for any break lengths or locations at nominal power level. Overpressure transients occur only for the low power channels as the average coolant condition at the outlet is still subcooled.

<u>Effect of Break Location and Length</u>

Cases 8 and 12 in Table-2 show the peak pressure predicted in the annulus and the pressure tube for a 2.25 m long outlet and inlet-end breaks to be around 14 MPa and 14.5 MPa respectively in Channel K01 at nominal flow and full-power conditions. Similar results are obtained for other channel as shown in Table 2 (cases 5 to 8 vs cases 9 to 12). The peak pressure obtained for the inlet break is higher compared to that for a break at the outlet for identical conditions. This effect can be attributed to coolant subcooling. As the coolant temperature at the inlet is lower than at the outlet, when the break occurs at the inlet, cooler fluid will first enter the annulus resulting in a higher peak pressure.

The peak transient pressure is highest for a full-length break (case 3), and hence is most limiting. This is due to the fact that the flow into the annulus is highest for a full length break and the flow has the highest average subcooling, as the coolant from both the inlet and the outlet-ends does not substantially increase in enthalpy by the time over pressurization occurs.

<u>Effect of Break Area</u>

The effect of break area has been studied by varying the valve discharge areas for a 2.25 m outlet break in Channel K01. The results obtained for three different break areas (Table 2, Cases 8, 13 and 14) indicated that the predicted peak pressure increases with increasing break area. The predicted peak pressure does not vary significantly when the break area is reduced, by about 25 percent, from 135 cm^2 to 100 cm^2 (Cases 8, 13). The peak pressure increases from 14 MPa to 15.5 MPa when the break area is increased, by about 25 percent, from 135 cm^2 to 175 cm^2 (Cases 8, 14). The results also show that the water-hammer peak occurs earlier for cases with a larger break area. With a larger break area, more coolant is discharged into the annulus resulting in a faster filling of the annulus.

Effect of Bearing Clearance Area

The effect of bearing clearances has been studied by varying the discharge area in the valve simulating the clearances. The results obtained for three different bearing clearances, for a 2.25 m outlet break in Channel K01, indicate that the predicted peak pressure decreases with increasing clearances area due to the increased discharge of coolant through the bearings (Cases 8, 15, 16). A doubling of the nominal bearing clearance area from 2.5 cm^2 to 5.0 cm^2 reduces the peak pressure by about 15 percent, while a reduction of the bearing area from 2.5 cm^2 to 1.25 cm^2 increases the peak pressure by about 20 percent. In order to verify this trend, two further cases were simulated with a full-length break in Channel K01 with bellows at both ends at 60 and 70 percent full power (Cases 25a and 26a). These results indicate that the effect of bearing clearances is not significant when the water-hammer pressure is already high.

Effect of Channel Power Level

The effect of channel power level has been studied by varying the operating power level in both the inner and outer zone Channels (J09 and A08). The selected power levels are sixty, seventy and eighty percent of full power, and the corresponding inlet header temperatures assumed are 253, 252 and 251^0 C respectively.

For Channel J09 two break geometries are considered, i.e., a full length break and an outlet end break. For the outlet end break (Cases 18, 19 and 20), the predicted peak pressures are 15 MPa, 18.5 MPa and 19 MPa corresponding to channel power levels of 80, 70 and 60 percent of nominal power respectively. For the full length break (Cases 22, 23 and 24), the corresponding predicted peak pressures are 16.7 MPa, 19.81 MPa and 20.79 MPa. The general increase in water-hammer pressure with decreasing channel power level is due to the increased subcooling of the discharged fluid. It is to be noted that there are no water-hammer pressures in the inner zone channels at 100 percent full power. However, at 80 percent full power, the pressure transients in these channels are similar to those predicted for outer zone channels at 100 percent full power (Cases 3 and 24). This trend of increasing water-hammer pressure with decreasing power is also observed for all full-length breaks (Cases 25 to 39). The peak water-hammer pressure appears to be limited to about 21 MPa.

Effect of Bellows Locations

Bruce NGS A Units 1, 2 and 3 have bellows only at one end, while the Bruce NGS B units and Bruce NGS A Unit 4 have bellows at both ends. In order to study the effect of bellows configuration, a few cases were considered, for channel J09 for various power levels, with the bellows either at inlet or outlet-end. The peak pressures obtained for Channel J09 with bellows at outlet-end (Cases 34, 35 and 36) and with bellows at inlet-end (Cases 37, 38 and 39) indicate that the bellows configuration does not influence the pressure transients significantly as compared with bellows at both ends (Cases 22, 23 and 24). The peak pressures are slightly higher when bellows are at the outlet-end. Similar trends in results are observed for outer zone Channel A08 as well (see Cases 28-30 vs 31-33).

Effect of Break Opening Time

In all the pressure transients simulated, a break opening time of 10 msecs was assumed. From the pressure transients presented in Figures 2 and 3, it can be seen that the annulus pressure does not change during the break opening time (initial 10 msecs). Hence, it is concluded that any reduction in break opening time will not affect the annulus pressure transient. However, when the break opening time is increased to 60 msecs (Case 17), the peak annulus pressure is seen to be lower due to the lower rate of initial discharge into the annulus.

Results and Discussion

Based on this sensitivity study, the influence of various parameters on the peak pressure can be generalized in terms of coolant subcooling and flow rate in the channel as follows:

(a) As the channel flows in Bruce NGS are very similar across the core, the peak pressure is higher for a low power channel in the outer zone due to higher subcooling. At 100 percent nominal power, there is no water-hammer pressurization in high power inner zone channels.

(b) An inlet break causes a larger water-hammer pressure than the same size break at the outlet of the fuel channel due to higher coolant subcooling at the inlet end.

(c) The maximum water-hammer pressure is obtained for a full-length break in the pressure tube. This can be attributed to the higher subcooling of the coolant being discharged into the annulus, as well as the larger discharge area.

(d) The peak water-hammer pressure increases with increasing break discharge area due to increasing flow.

(e) The peak water-hammer pressure decreases with increasing bearing clearance areas.

(f) For a given channel power the predicted water-hammer pressure significantly increases when the channel power level decreases. This can be attributed to the higher average coolant subcooling as power decreases.

(g) The peak pressures are slightly higher when bellows are located at the outlet-end for units with bellows only at one end.

(h) When the break opening time is increased, (from 10 to 60 msecs) the predicted peak annulus pressure is seen to be lower (case 17). However, for irradiated pressure tubes the break opening time of 10 msec is considered appropriate.

CALANDRIA TUBE RESPONSE TO ANNULUS PRESSURE TRANSIENTS

The structural response of the CT to the MINI-SOPHT predicted annulus pressure transients is presented in this section. The method of accounting for the strain attenuation effect on pressure transients is given in Reference 2. This methodology has been validated by comparison with the results from the full-scale pressure tube burst tests reported in References 4 to 7. The response of the CT to the pressure transients simulated is presented first. Based on this response, the estimated CT strength margins to failure are presented for a typical PT failure.

The CT strain attenuation effect (based on the material strength data given Table 1) is reported here for all the simulated cases in Table 2. The predicted peak pressure and the plastic strain of the CT are shown in Table 3 for a Bruce CT with nominal irradiated tube material properties (given in Reference 8) and without accounting for anisotropy effects. These results indicate that the CT response is mainly elastic in the majority of the cases simulated except for the reduced power cases. The maximum estimated plastic strain is around 0.85 percent for the limiting case of a full-length break in the outer zone low power Channel A08 at 60 percent full-power operation. (Case 28)

Experimental results (Reference 8) have shown that the biaxial strength of the CT is always higher than the uniaxially measured values due to anisotropy of Zr-2 material; however, it is difficult to quantify the anisotropy parameters precisely. In order to conservatively account for the strengthening effect, the yield and ultimate tensile strength are increased by 20 percent (the lowest experimentally observed increase in strength) in strain attenuation calculations. The predicted results with these increased material strength parameters are shown in Table 4 for all the cases. These results indicate that the peak corrected pressures are higher while the predicted plastic strain values during the transient are lower (compare Tables 3 and 4).

Margin to Calandria Tube Failure in Reactor

The methodology of evaluating the calandria tube strength margin in the event of a sudden pressure tube failure for the reactor cases is presented in Ref 3. Using this methodology the margin to failure is calculated for the CTs in the Bruce reactors. In all cases presented, a 20% strengthening due to anisotropy is assumed. As in Ref 3, the criteria used are:

(1) A strain based criterion which assumes that the CT fails when the average plastic strain reaches 0.1 percent during the transient.

(2) A stress based criterion which assumes that the CT fails when the hoop stress in the CT exceeds the dynamic ultimate tensile strength.

The low ductility strain (0.1 percent) limit criterion is used to cover failures resulting from defective calandria tube welds or other anomalies. For the stress criterion the CT is assumed sufficiently ductile, and hence, there is no imposed limit on plastic strain. Similarly, to illustrate the tube-to-tube strength variation, both the nominal expected values and the lower bound values of CT material properties (given in Table 1) are considered. The lower bound values are obtained by considering the mean measured values of unirradiated materials and by assuming that the spread of yield and ultimate tensile strengths (i.e. the ratio of the mean to the minimum value) in the irradiated condition is identical to that of unirradiated material. This is very conservative as it ignores the observed narrower spread of these material properties towards the mean in irradiated material (i.e., irradiation tends to reduce the spread in material strength from tube to tube).

Again as in Ref 3, the margin to failure is estimated for the break located either at the inlet end or outlet end and for the full length break. The strength margins calculated, for the three breaks with the above two criteria, for Bruce reactors is given in Table 5. The effect of garter spring indentation is also accounted for in the steady-state phase by lowering the margin as in Ref 3. Typical results of the calculations for Channel K01 at full-power given in Table 5, show that a large margin to failure exists for both lower bound strength and nominal irradiated strength calandria tube for a G-16 type of outlet-end failure. For this break size, the limiting failure margin is always obtained for the steady-state rather than the transient phase when garter spring indentation effects are included. Note that the steady state annulus pressure is not dependent on break length and hence the margin to failure is identical for all breaks shown in Table 5.

For an inlet-end break and for a full-length break, the failure margins for a lower bound strength tube are seen to be very small or negative based on a 0.1 percent failure criterion. The corresponding failure margins for a nominal tube is positive. Thus for the low ductility failure criterion (0.1 percent plastic strain) the limiting failure margin for a full-length break and for an inlet-end break are obtained for the transient rather than the steady-state loading phase. For the higher ductility stress failure criterion large margins to failure are again obtained.

It is reiterated that the lower bound strength is unrealistic since tube strengths approach approximately the same nominal strength after several years irradiation. It is also reiterated that garter spring indentation is not expected to significantly affect the margin to failure. Finally the low ductility failure can be considered unlikely or of low probability as it assumes a defect in the weld. Consequently the margins predicted based on nominal strength and stress criterion are realistic. The expected failure margins are denoted by asterisks in Table 5 for the transient and steady state.

CONCLUSIONS

The issue of CT survivability in the event of a PT break in Bruce NGS has been examined in detail. The water-hammer type overpressure transient causes plastic straining of the CT which, in turn, has a feedback effect of reducing the peak pressure. A detailed thermal-hydraulic analysis of the expected pressure transients and the strain feedback effect is presented. In the final stage, the CT is subjected to a steady-state loading which is close to the mean of the inlet and outlet header pressure.

Based on the results of the analyses, it is concluded that for Bruce NGS:

(a) The CT will survive an outlet-end PT failure (such as G-16) under normal operating conditions with a large margin to failure for the full range of tube strength and ductility expected in reactor.

(b) The CT will survive a full-length (6 metre) PT failure under normal operating conditions with a large, but reduced, margin to failure for tubes of expected (nominal) strength free of weld or other defects. The shorter the PT rupture, the greater the margin to failure.

(c) Should a full-length (6 metre) rupture occur in a channel with a CT weld or other defect such that low ductility failures can occur, the integrity of the CT will be challenged.

(d) Garter spring indentation of the CT can potentially, but not necessarily reduce the margin to CT failure.

REFERENCES

(1) Kundurpi, P.S., and Muzumdar, A.P., "Structural Response of Calandria Tube to a Spontaneous Rupture of the Pressure Tube", International J. Pressure Vessel and Piping 31 (1988) 241-253.

(2) Kundurpi, P.S., and Muzumdar, A.P., "Sensitivity Studies of Calandria Tube Integrity in the Event of Pressure Tube Failure". Paper presented at the 9th Annual CNS Conference at Winnipeg, June 1988.

(3) Kundurpi P.S. et. al. "Pickering NGS: Assessment of Calandria Tube Integrity Following a Sudden Pressure Tube Rupture", Paper Presented at the 10th CNS Conference at Ottawa. June 1989.

(4) Muzumdar, A.P., et al, "Experimental Program to Determine the Consequences of Pressure Tube Rupture in Reactors". Paper presented at the International ANS/ENS Topical Meeting on "Thermal Reactor Safety", San Diego, California, February 1986.

(5) Muzumdar, A.P., et al, "Simulation of CANDU Pressure Tube Rupture Experiments". Paper presented at the International ANS/ENS Topical Meeting on "Thermal Reactor Safety", San Diego, California, February 1986.

(6) Hadaller, G.I., and Muzumdar, A.P., "Progress on an Experimental Program to Determine the Consequences of Pressure Tube Rupture in CANDU Reactors". Paper presented at the 8th Annual CNS Conference, Saint John, NB, June 1987.

(7) Hadaller, G.I., and Muzumdar, A.P., "Full-Scale Calandria Tube Burst Tests at Fast Pressurization Rates". Paper presented at the 9th Annual CNS Conference at Winnipeg, June 1988.

(8) Ells, C.E., et al, "The Strength of CANDU Calandria Tubes", COG Report RC-52 COG-90-39 (April 1990).

TABLE 1

Geometries and Channel Data for J09

Channel Power - 6.22 MW
Nominal Flow - 24.4 kg/sec
Inlet Temperature - 251°C

Inlet Header Pressure = 10.56 MPa
Outlet Header Pressure = 9.4 MPa

	D(mm)	L(m)	V(m^3)	Flow Area (m^2)	k
Inlet Feeder	62.94	9.7674	3.04E-2		
Inlet Feeder	48.89	0.2988	5.62E-4		
Inlet End Fitting	74.0	0.2476		.00342	3.03
Channel	7.60	5.94 m		.00352	9.7944
Outlet End Fitting	74.0	0.2476		.00342	3.03
Outlet Feeder	62.941	5.156	2.126E-2		
Outlet Feeder	74.168	8.936	3.861E-3		

Geometries and Channel Data for K01

Channel Power - 4.215 MW
Nominal Flow - 23.91 kg/sec
Inlet Temperature - 265°C

Inlet Header Pressure = 10.501 MPa
Outlet Header Pressure = 9.40 MPa

	D(mm)	L(m)	V(m^3)	A(m^2)	k
Inlet Feeder	48.895	8.2338	1.547E-2		
Inlet Feeder	62.941	5.2478	1.632E-3		
Inlet End Fitting	74.2	0.2476		.00342	3.03
Channel	7.6	5.94 m		.00352	9.7944
Outlet End Fitting	74.2	0.2476		.00342	3.03
Outlet Feeder	62.94	3.7103	1.156E-2		
Outlet Feeder	74.17	12.560	5.426E-2		

Geometry and Material Data for Calandria Tube

Inner diameter = 129 mm   Thickness = 1.37 mm

At room temperature, assumed Properties:
Nominal properties: σ_y = 580 MPa, σ_{UTS} = 660 MPa
Lower bound values σ_y = 540 MPa σ_{UTS} = 580 MPa

TABLE 2

Simulation Matrix of Cases Considered and Results of Thermal Hydraulic Simulation

Test Case	Location of Break	Break Size (m)	Channel	Bearing Area	Break Discharge Area cm^2	Power Level (%)	Bellows Configuration	Peak Pressure (MPa)	Pressure Pulse Width (ms)
1	Full Length	5.94	J09	Nominal	390	100	Both Ends	9.7	-
2	Full Length	5.94	L10	Nominal	390	100	Both Ends	9.7	-
3	Full Length	5.94	A08	Nominal	390	100	Both Ends	16.0	54
4	Full Length	5.94	K01	Nominal	390	100	Both Ends	15.0	55
5	Outlet End	2.25	J09	Nominal	135	100	Both Ends	9.7	-
6	Outlet End	2.25	L10	Nominal	135	100	Both Ends	9.7	-
7	Outlet End	2.25	A08	Nominal	135	100	Both Ends	14.8	50
8	Outlet End	2.25	K01	Nominal	135	100	Both Ends	14.0	50
9	Inlet End	2.25	J09	Nominal	135	100	Both Ends	9.7	-
10	Inlet End	2.25	L10	Nominal	135	100	Both Ends	9.7	-
11	Inlet End	2.25	A08	Nominal	135	100	Both Ends	15.4	50
12	Inlet End	2.25	K01	Nominal	135	100	Both Ends	14.5	50
13	Outlet End	2.25	K01	Nominal	100	100	Both Ends	14.0	50
14	Outlet End	2.25	K01	Nominal	175	100	Both Ends	16.0	50
15	Outlet End	2.25	K01	1/2 Nominal	135	100	Both Ends	17.0	50
16	Outlet End	2.25	K01	2 Nominal	135	100	Both Ends	12.0	50
17	Outlet End (Slow Opening of 60 ms)	5.94	K01	Nominal	390	100	Both Ends	13.0	50
18	Outlet End	2.25	J09	Nominal	135	60	Both Ends	19.1	51
19	Outlet End	2.25	J09	Nominal	135	70	Both Ends	18.5	50
20	Outlet End	2.25	J09	Nominal	135	80	Both Ends	15.0	51

TABLE 2 (Cont'd)

Simulation Matrix of Cases Considered and Results of Thermal Hydraulic Simulation

Test Case	Location of Break	Break Size (m)	Channel	Bearing Area	Break Discharge Area cm^2	Power Level (%)	Bellows Configuration	Peak Pressure (MPa)	Pressure Pulse Width (ms)
22	Full Length	5.94	J09	Nominal	390	60	Both Ends	20.79	55
23	Full Length	5.94	J09	Nominal	390	70	Both Ends	19.81	53
24	Full Length	5.94	J09	Nominal	390	80	Both Ends	16.70	54
25	Full Length	5.94	K01	Nominal	390	60	Outlet End	20.5	54
25(a)	Full Length	5.94	K01	1/2 Nominal	390	60	Outlet End	20.71	54
26	Full Length	5.94	K01	Nominal	390	70	Outlet End	18.0	54
26(a)	Full Length	5.94	K01	1/2 Nominal	390	70	Outlet End	20.12	54
27	Full Length	5.94	K01	Nominal	390	80	Outlet End	16.1	54
28	Full Length	5.94	A08	Nominal	390	60	Outlet End	21.7	54
29	Full Length	5.94	A08	Nominal	390	70	Outlet End	18.5	54
30	Full Length	5.94	A08	Nominal	390	80	Outlet End	16.9	54
31	Full Length	5.94	A08	Nominal	390	60	Inlet End	20.3	51
32	Full Length	5.94	A08	Nominal	390	70	Inlet End	17.1	51
33	Full Length	5.94	A08	Nominal	390	80	Inlet End	15.7	51
34	Full Length	5.94	J09	Nominal	390	60	Outlet End	20.9	54
35	Full Length	5.94	J09	Nominal	390	70	Outlet End	17.2	54
36	Full Length	5.94	J09	Nominal	390	80	Outlet End	15.03	54
37	Full Length	5.94	J09	Nominal	390	60	Inlet End	19.51	54
38	Full Length	5.94	J09	Nominal	390	70	Inlet End	17.80	54
39	Full Length	5.94	J09	Nominal	390	80	Inlet End	14.52	54

TABLE 3

Corrected Annulus Peak Pressure and CT Plastic Strain for Nominal Material Properties

Case No.	SOPHT Pressure (MPa)	Pulse Width (ms)	Peak Corrected Pressure (MPa)	Plastic Strain (%)
1	9.7	-	-	-
2	9.7	-	-	-
3	16.0	54	11.85	0.295
4	15.0	55	11.7	0.208
5	9.7	-	-	-
6	9.7	-	-	-
7	14.8	50	11.71	0.185
8	14.0	50	11.57	0.12
9	9.7	-	-	-
10	9.7	-	-	-
11	15.4	50	11.76	0.25
12	14.5	50	11.62	0.15
13	14.0	50	11.55	0.115
14	16.0	50	11.75	0.28
15	17.0	50	11.97	0.383
16	12.0	50	-	-
17	13.0	50	11.32	0.052
18	19.1	51	12.12	0.592
19	18.5	50	12.08	0.529
20	15.0	51	11.7	0.20
22	20.79	55	12.19	0.761
23	19.81	53	12.15	0.661
24	16.70	54	11.91	0.359
25	20.5	54	12.18	0.73
26	18.0	54	12.09	0.48
27	16.1	54	11.85	0.30
28	21.7	54	12.25	0.85
29	18.5	54	12.05	0.535
30	16.9	54	11.93	0.378
31	20.3	51	12.20	0.206
32	17.1	51	11.98	0.393
33	15.7	51	11.82	0.265
34	20.9	54	12.21	0.77
35	17.2	54	11.96	0.406
36	15.03	54	11.71	0.209
37	19.51	54	12.12	0.633
38	17.80	54	12.02	0.463
39	19.52	54	11.63	0.168

Note: Fluid temperature in all cases was 285°C.
Reference pressure was 9 MPa.

TABLE 4

Corrected Peak Annulus Pressure and CT Plastic Strain with Biaxial Effect Included (Yield Stress and Ultimate Tensile Strength 20 % above Nominal Value To Account for Biaxial Effect)

Case No.	SOPHT Pressure (MPa)	Pulse Width (ms)	Peak Corrected Pressure (MPa)	Plastic Strain (%)
1	9.7	-	-	-
2	9.7	-	-	-
3	16.0	54	13.59	0
4	15.0	55	12.93	0
5	9.7	-	-	-
6	9.7	-	-	-
7	14.8	50	12.78	0
8	14.0	50	12.27	0.0
9	9.7	-	-	-
10	9.7	-	-	-
11	15.4	50	13.19	0.0
12	14.5	50	12.0	0.0
13	14.0	50	12.27	0.0
14	16.0	50	13.58	0.0
15	17.0	50	14.24	0.0
16	12.0	50	10.90	0.0
17	13.0	50	11.62	0.0
18	19.1	51	15.03	0.11
19	18.5	50	14.91	0.06
20	15.0	51	12.9	0.0
22	20.79	55	15.24	0.26
23	19.81	53	15.13	0.17
24	16.70	54	14.04	0.0
25	20.5	54	15.21	0.233
26	18.0	54	14.73	0.032
27	16.1	54	13.6	0.0
28	21.7	54	15.34	0.343
29	18.5	54	14.87	0.066
30	16.9	54	14.87	0.0
31	20.3	51	15.21	0.2
32	17.1	51	14.3	0.0
33	15.7	51	13.39	0.0
34	20.9	54	15.26	0.269
35	17.2	54	14.36	0.002
36	15.03	54	12.9	0.0
37	19.51	54	15.07	0.147
38	17.80	54	14.67	0.02
39	14.52	54	12.62	0.0

TABLE 5

Calandria Tube Percent Margin to Failure
(For Various Failure Criteria Following a
Sudden Pressure Tube Failure in Channel K01 at 100% Power)

Failure Criterion	Inlet End Break		Outlet End Break		Full Length Break	
	Lower Bound Strength	Nominal Strength	Lower Bound Strength	Nominal Strength	Lower Bound Strength	Nominal Strength
Transient Loading Phase						
0.1% Plastic Strain during transient	-1.9	23.3	7.8	35.7	0.006	26.6
Stress exceeds ultimate tensile strength during transient	57.1	73.3*	72.8	90.7*	61.3	78.5*
Steady State Loading Phase						
Hoop stress exceeds ultimate tensile strength during steady state	8	23**	8	23**	8	23**
The above criterion with allowance for realistic garter spring indentation	0.7	15.7	0.7	15.7	0.7	15.7

* Expected margin to failure during transient.
** Expected margin to failure during steady state.

Schematic Nodalization

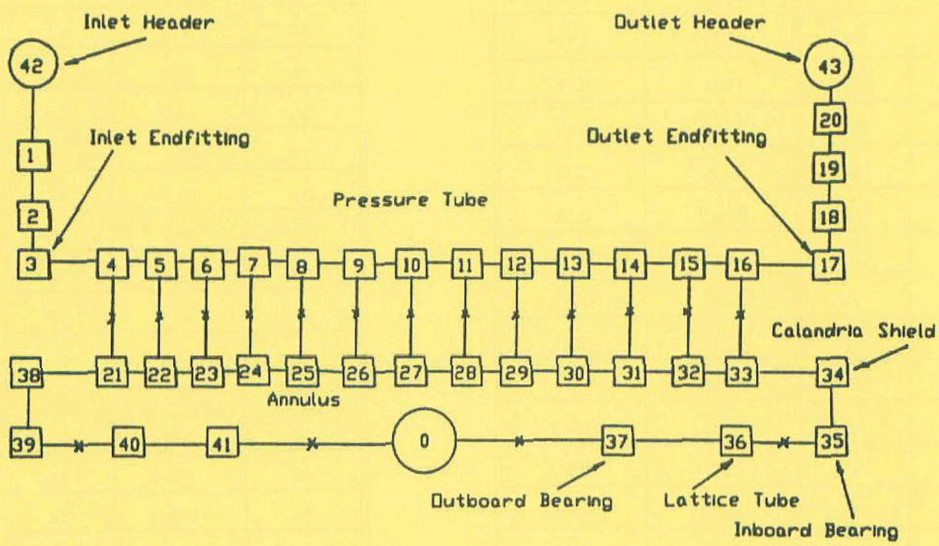

FIGURE 1 : Schematic nodalization of the header to header model in MINI-SOPHT

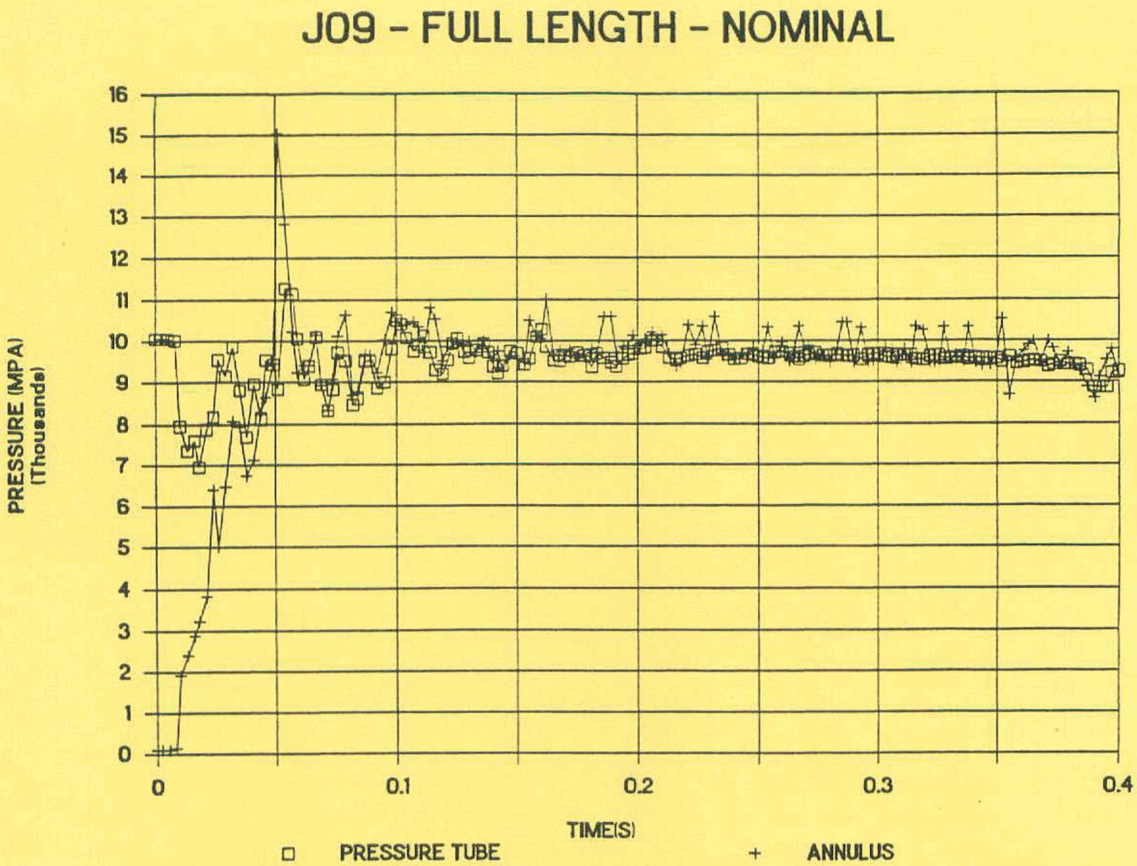

Figure 2 : Pressure transient in the inner channel J09, for a full length break in the pressure tube, at nominal condition

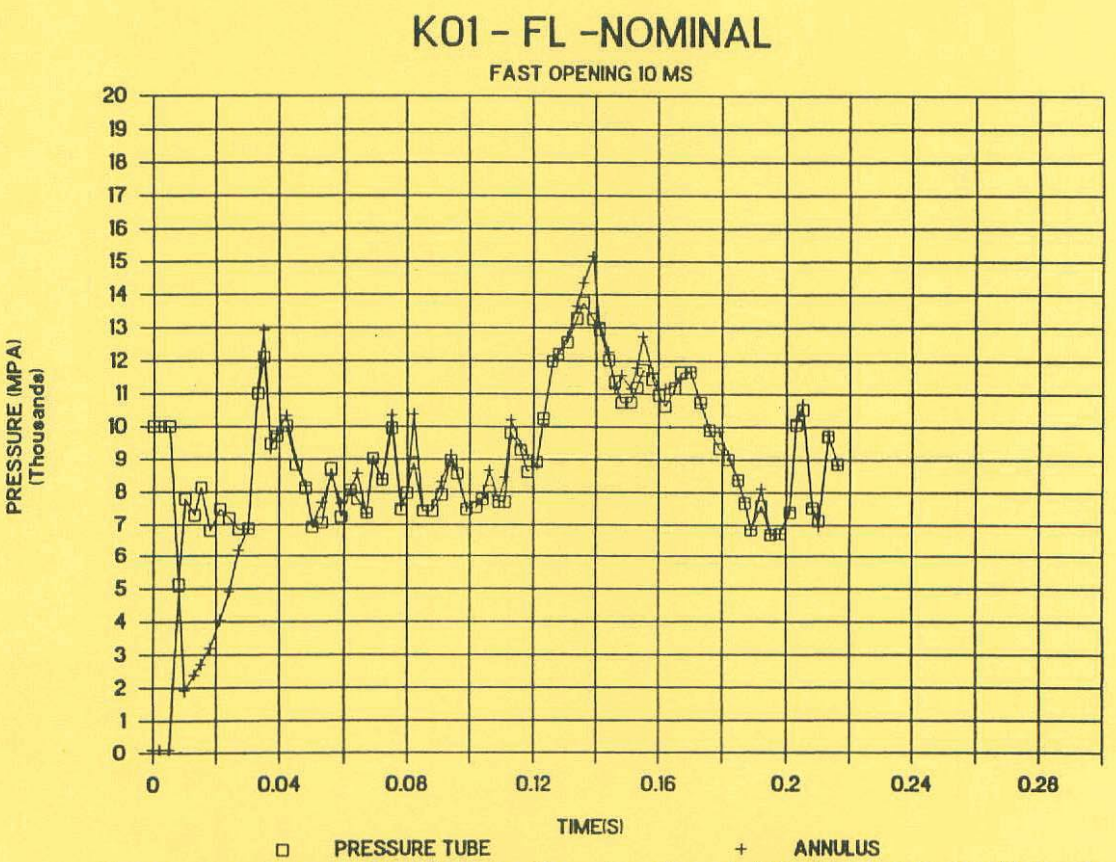

Figure 3 : Pressure transient in the outer channel K01, for a full length break in the pressure tube, at nominal condition